ISSN: 2664-9640

State-feedback control of quadrotors based on periodic event-triggered mechanism

Dezhi Kong*, Dong Zhang, Ziyou Zhang, Yuhe Chen, Guangyu Jia and Xia Chen

School of Information and Control Engineering, Qingdao University of Technology, Qingdao, 266525, China

* Corresponding author Email: sdzz980915@163.com

Abstract

Quadrotors are easily affected by various adverse factors such as wind disturbance during flight, which leads to its constant adjustment of flight attitude and position information, resulting in a large waste of communication resources between ground stations and quadrotors, especially in the case of drone swarm. In the case of limited communication resources, in order to reduce the calculation and communication burden of the system, this paper designs a control scheme which combines the periodic event-triggered mechanism with the quadrotor state-feedback controller. Firstly, the mathematical model of the quadrotor is established and linearized. Secondly, the state-feedback controller is combined with periodic event-triggered mechanism, and its stability is proved. Then, the joint design criteria of feedback gain matrix and event condition parameters expressed by linear matrix inequalities are designed. The simulation results show that the periodic event-triggered control scheme can effectively save the communication resources between the ground station and quadrotors , and maintain the quadrotor's stable flight.

Keywords

Quadrotor, communication resources, periodic event-triggered control, linear matrix inequalities.

1. Introduction

Quadrotors use air power to overcome its own weight, and can fly autonomously or remotely. It has the characteristics of flexibility, vertical takeoff and landing, and fixed point hovering [1]. Quadrotors can effectively carry out the tasks of traffic monitoring, terrain mapping and material transportation, and have broad application prospects in national defense construction [2]. In the practical application of quadrotor, the effective utilization of communication resources is a problem worthy of attention. Many theoretical studies have shown that event-triggered control can effectively reduce communication amount. Therefore, it is of practical significance to apply the event-triggered strategy to the information exchange between the ground station and quadrotors.

In event-triggered control algorithms, the control law updates based on the new sampled state only if the trigger condition is satisfied. [3] designed an event-triggered reinforcement learning (RL) control strategy to solve the problem that the quadrotor has complex dynamic characteristics and is difficult to model accurately. Based on the distributed event-triggered strategy, the triggering condition of the consensus based formation control is derived, which is used to protect the privacy of the formation control scheme in a limited time [4]. In the framework of zero-space behavior Control (NSBC), [5] proposed an event-triggered mechanism to determine whether intervention is necessary and when to intervene, so that UAVs can intervene in the tasks of unmanned vehicles. [6] studied the event-triggered control of

ISSN: 2664-9640

saturated state-feedback and observe-based saturatedfeedback linear systems, respectively. In [7], a distributed event-triggered technique is proposed for a class of state-feedback controllers for linear systems. An event-triggered discrete-time neural control was investigated by using a discrete-time interference observer (DTDO), thus applying it to the quadrotor [8]. A position tracking control method based on event-triggered mechanism was proposed for the quadrotor with multi-state delay and external interference [9]. In [10], the issue of event-triggered output-feedback control for UAVs over cognitive radio (CR) networks was studied.

In event-triggered control, event conditions must be verified to determine the release time of the control task. Furthermore, in order to avoid Zeno phenomenon, the time interval between events should be strictly positive and most references avoid Zeno phenomenon by introducing additional conditions. the periodic event-triggered control can avoid the Zeno phenomenon, which uses a fixed verification cycle to evaluate the event conditions of periodic event-triggered control. In this aspect, [11] have proved that the introduction of validation cycles can enable periodic eventtriggered controls to produce positive interaction times and save more computing and communication resources. Therefore, for the quadrotor system, a control scheme combining the periodic event-triggered mechanism and the quadrotor state-feedback is designed based on the joint design problem of the state-feedback gain matrix and the event condition parameters.

The remaining structure of the article is as follows. In section 2, the quadrotor system model is established and linearized. In Section 3, a control scheme combining state-feedback controller and periodic event-triggered control is designed. In Section 4, the proposed control scheme is simulated. Section 5 gives the conclusion.

2. Mathematical model and linearization of quadrotors

The schematic diagram of the quadrotor model is shown in Figure 1 . The Earth's inertial coordinate system (e system) and body coordinate system (b system) are defined to describe the freedom of the moving rigid body of the quadrotor. O_e is the axis origin, $\{X_b, Y_b, Z_b\}$ represents the body coordinate system, O_b is the coordinate origin, which coincides with the center of the quadrotor cross structure, and the Earth coordinate system (e system) is an inertial right-handed reference system, which is represented by $\{X_e, Y_e, Z_e\}$. In order to facilitate the derivation of the mathematical model of the quadrotor system, the following assumptions need to be made:

(a) The body of the quadrotor system is rigid and symmetrical.

(b) The quadrotor's center of mass coincides with the origin of the coordinate system.

2.1. Nonlinear model of quadrotors

According to Euler's rotation theorem, the rotation matrix from the body coordinate system to the inertial coordinate system can be expressed as

$$R_{\mathrm{b}}^{\mathrm{e}} = \begin{bmatrix} \mathrm{c}_\theta \mathrm{c}_\psi & \mathrm{c}_\psi \mathrm{s}_\phi \mathrm{s}_\theta - \mathrm{c}_\phi \mathrm{s}_\psi & \mathrm{c}_\phi \mathrm{c}_\psi \mathrm{s}_\theta + \mathrm{s}_\phi \mathrm{s}_\psi \\ \mathrm{c}_\theta \mathrm{s}_\psi & \mathrm{s}_\phi \mathrm{s}_\theta \mathrm{s}_\psi + \mathrm{c}_\phi \mathrm{c}_\psi & \mathrm{c}_\phi \mathrm{s}_\theta \mathrm{s}_\psi - \mathrm{c}_\psi \mathrm{s}_\phi \\ -\mathrm{s}_\theta & \mathrm{s}_\phi \mathrm{c}_\theta & \mathrm{c}_\phi \mathrm{c}_\theta \end{bmatrix} \tag{1}$$

where $\mathrm{c}_\iota = \cos(\iota), \mathrm{s}_\iota = \sin(\iota)$.

ISSN: 2664-9640

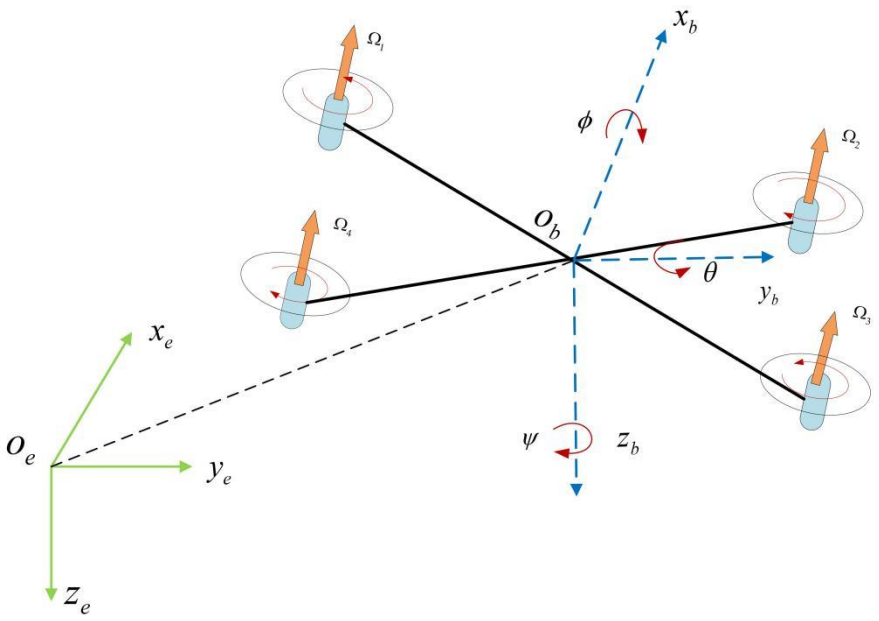

Figure 1: Diagram of the quadrotor system

The relationship between Euler angle vector $\Theta=\left[\phi,\theta,\psi\right]^T$ and the rotational angular velocity vector $\omega=\left[\omega_x,\omega_y,\omega_z\right]^T$ of the quadrotor are as follows:

$$\dot{\Theta}=\begin{bmatrix}\dot{\phi}\\ \dot{\theta}\\ \dot{\psi}\end{bmatrix}=G_1\omega, G_1=\begin{bmatrix}1 & s_\phi t_\theta & c_\phi t_\theta\\ 0 & c_\phi & -s_\phi\\ 0 & \frac{s_\phi}{c_\theta} & \frac{c_\phi}{c_\theta}\end{bmatrix} \tag{2}$$

where $t_\iota=\tan(\iota)$.

Mainly, the quadrotor is controlled near its equilibrium points where the Euler angles are small ($<15°$). Thus, (2) can be simpled as $\dot{\Theta}=\omega, G_1=I_{3\times3}$ for small angles.

Then, the translational dynamics of the quadrotor is

$$\begin{bmatrix}\ddot{x}\\ \ddot{y}\\ \ddot{z}\end{bmatrix}=\begin{bmatrix}-\left(c_\phi s_\theta c_\psi+s_\phi s_\psi\right)u_z/m\\ -\left(c_\phi s_\theta s_\psi-s_\phi c_\psi\right)u_z/m\\ -\left(c_\phi c_\theta\right)u_z/m+g\end{bmatrix} \tag{3}$$

where $\xi=\left[x,y,z\right]^T$ and $\xi=\left[x,y,z\right]^T$ are the position and speed of the quadrotor, respectively. m is the weight of the quadrotor and g is the acceleration of gravity.

The attitude dynamics is

$$\begin{bmatrix}\ddot{\phi}\\ \ddot{\theta}\\ \ddot{\psi}\end{bmatrix}=\begin{bmatrix}\dot{\theta}\,\dot{\psi}\left(J_y-J_z\right)/J_x+\dot{\theta}\,\Omega_r J_r/J_x+u_\phi/J_x\\ \dot{\phi}\,\dot{\psi}\left(J_z-J_x\right)/J_y-\dot{\phi}\,\Omega_r J_r/J_y+u_\theta/J_y\\ \dot{\phi}\,\dot{\theta}\left(J_x-J_y\right)/J_z+u_\psi/J_z\end{bmatrix} \tag{4}$$

where $J=\left[J_x,J_y,J_z\right]$ is the quadrotor moment vector of inertia, J_r is the inertia moment of propeller, Ω_r is the relative rotor speed.

ISSN: 2664-9640

The corresponding control input is

$$u=\begin{bmatrix}u_z\\u_\phi\\u_\theta\\u_\psi\end{bmatrix}=\begin{bmatrix}c_T & c_T & c_T & c_T\\ \frac{\sqrt{2}}{2}lc_T & -\frac{\sqrt{2}}{2}lc_T & -\frac{\sqrt{2}}{2}lc_T & \frac{\sqrt{2}}{2}lc_T\\ \frac{\sqrt{2}}{2}lc_T & \frac{\sqrt{2}}{2}lc_T & -\frac{\sqrt{2}}{2}lc_T & -\frac{\sqrt{2}}{2}lc_T\\ d_R & -d_R & d_R & -d_R\end{bmatrix}\begin{bmatrix}\Omega_1^2\\\Omega_2^2\\\Omega_3^2\\\Omega_4^2\end{bmatrix} \tag{5}$$

u_z is the total pulling force and $u_\phi \sim u_\psi$ are the torque generated in the corresponding direction. c_T is the thrust coefficient, d_R is the torque coefficient, l is the arm length of the quadrotor, Ω_i is the propeller speed corresponding to the number $i=1,2,3,4$.

2.2. Linearization of quadrotor model

It can be seen from equations (3) and (4) that the quadrotor system is a typical nonlinear system with the characteristics of underdrive, multi-coupling and high order, which makes the analysis and controller design of the quadrotor system complicated. To facilitate the controller design, the nonlinear model is usually appropriately :

$$\begin{aligned} m\ddot{x}&=-u_z(\mathrm{c}_\phi \mathrm{s}_\theta \mathrm{c}_\psi+\mathrm{s}_\phi \mathrm{s}_\psi); & J_x\ddot{\phi}&=u_\phi\\ m\ddot{y}&=-u_z(\mathrm{c}_\phi \mathrm{s}_\theta \mathrm{s}_\psi-\mathrm{s}_\phi \mathrm{c}_\psi); & J_y\ddot{\theta}&=u_\theta\\ m\ddot{z}&=-u_z\,\mathrm{c}_\phi \mathrm{c}_\theta+mg; & J_z\ddot{\psi}&=u_\psi \end{aligned} \tag{6}$$

This paper will use a simplified linear model for discussion. Using the small Angle theory, the following formula can be obtained [12]

$$\sin\phi\approx\phi,\cos\phi\approx1,\sin\theta\approx1,\cos\theta\approx1. \tag{7}$$

Bring equation (7) into equation (6) to get

$$\begin{bmatrix}\ddot{x}\\\ddot{y}\\\ddot{z}\\\ddot{\phi}\\\ddot{\theta}\\\ddot{\psi}\end{bmatrix}=\begin{bmatrix}-\theta g\\ \phi g\\ -(u_z-mg)/m\\ u_\phi/J_x\\ u_\theta/J_y\\ u_\psi/J_z\end{bmatrix} \tag{8}$$

The quadrotor system (2.8) expressed in matrix form is

$$\begin{bmatrix}\dot{x}\\\dot{y}\\\dot{z}\\\ddot{x}\\\ddot{y}\\\dot{z}\\\dot{\phi}\\\dot{\theta}\\\dot{\psi}\\\ddot{\phi}\\\ddot{\theta}\\\ddot{\psi}\end{bmatrix}=\begin{bmatrix}0&0&0&1&0&0&0&0&0&0&0&0\\0&0&0&0&1&0&0&0&0&0&0&0\\0&0&0&0&0&1&0&0&0&0&0&0\\0&0&0&0&0&0&0&-g&0&0&0&0\\0&0&0&0&0&0&g&0&0&0&0&0\\0&0&0&0&0&0&0&0&0&0&0&0\\0&0&0&0&0&0&0&0&0&1&0&0\\0&0&0&0&0&0&0&0&0&0&1&0\\0&0&0&0&0&0&0&0&0&0&0&1\\0&0&0&0&0&0&0&0&0&0&0&0\\0&0&0&0&0&0&0&0&0&0&0&0\\0&0&0&0&0&0&0&0&0&0&0&0\end{bmatrix}\begin{bmatrix}x\\y\\z\\\dot{x}\\\dot{y}\\\dot{z}\\\phi\\\theta\\\psi\\\dot{\phi}\\\dot{\theta}\\\dot{\psi}\end{bmatrix}+\begin{bmatrix}0&0&0&0\\0&0&0&0\\0&0&0&0\\0&0&0&0\\0&0&0&0\\-1/m&0&0&0\\0&0&0&0\\0&0&0&0\\0&0&0&0\\0&1/J_x&0&0\\0&0&1/J_y&0\\0&0&0&1/J_z\end{bmatrix}\begin{bmatrix}\hat{u}_z\\u_\phi\\u_\theta\\u_\psi\end{bmatrix}, \tag{9}$$

where $\hat{u}_z=u_z-mg$.

ISSN: 2664-9640

3. Periodic event-triggered state-feedback control of quadrotors

Event-triggered control updates the state and control quantities according to the control performance requirement. If the trigger condition is satisfied at a certain point, it means that the event has been triggered and the control task is immediately executed. Therefore, the number of control tasks can be effectively reduced and computational and communication resources can be significantly saved on the basis of ensuring the performance of closed-loop systems.

3.1. Event-triggered mechanism

3.1.1. Continuous event-triggered mechanism

The error is expressed as

$$e(t)=\tilde{x}(t)-\tilde{x}(t_k),t\in[t_k,t_{k+1}). \tag{10}$$

where t_k is the moment when the sensor obtains data from the controlled object and transmits the data to the controller, $t_0=0$; $\tilde{x}(t_k)$ and $\tilde{x}(t)$ are the state of the system at the last trigger moment and current state, respectively.

In many literatures, $e(t)$ can be calculated online according to the real-time measurement state $\tilde{x}(t)$, and trigger sampling is carried out directly when the event-triggered conditions are met.

Event-triggered conditions are classified into fixed threshold event-triggered conditions and relative threshold event-triggered conditions. The expressions are as follows

$$t_{k+1}=t_k+\min\left\{t\,|\,\|e(t)\|\geq\delta\right\} \tag{11}$$

$$t_{k+1}=t_k+\min\left\{t\,|\,\|e(t)\|\geq\delta\|\tilde{x}\|\right\} \tag{12}$$

where δ is the given constant. As can be seen from equation (11) and (12) whether the current data can be transmitted depends on the event-triggered scheme. However, continuous event-triggered mechanisms require special hardware to continuously measure system state.

3.1.2. Discrete event-triggered mechanism

Compared to the continuous event-triggered scheme mentioned above, the discrete event-triggered one only measures the state and calculates the deviation in a fixed sampling period, so no additional hardware is required for continuous measurement and calculation. An early discrete event-triggered mechanism was proposed by Heemels, also known as periodic event-triggered control [13] .

The periodic event-triggered control strategy combines the traditional periodic data sampling control with the event-triggered control to periodically sample and exchange the data of the sensor and controller [14]. In addition, a model-based periodic event is proposed in [15]. Compared with the open-loop event triggering control scheme, closed-loop modeling method is adopted for trigger control. It can significantly reduce the number of signals transmitted compared to traditional event-triggered control with a baseline strategy, and can increase the battery life of wireless devices if the energy consumed by computation is less than that consumed by communication.

Therefore, the periodic event triggering control mechanism is as follows

$$t_{k+1}h=t_kh+\min_{l\geq1}\left\{lh\,|\,e^T(i_kh)\Phi e(i_kh)\geq\Psi\tilde{x}^T(i_kh)\Phi\tilde{x}(i_kh)\right\}, \tag{13}$$

where $\Psi>0$ is the given scalar parameter, Φ is the positive definite weighted trigger matrix to be solved, $i_kh=t_kh+lh, e(i_kh)=\tilde{x}(i_kh)-\tilde{x}(t_kh)$. As can be seen from equation (13), the transmission

ISSN: 2664-9640

of the event is determined by $e_k(i_k h)$ and the current state $\tilde{x}(t_k h)$, and the event is triggered when the conditions in equation (13) are met.

To sum up, the periodic event-triggered mechanism makes up for the defect of the traditional event-triggered strategy that requires continuous state detection, and only measures the state and calculates the deviation within a fixed sampling period, so the transmission times of the signal can be reduced.

3.2. Periodic event-triggered and state-feedback control

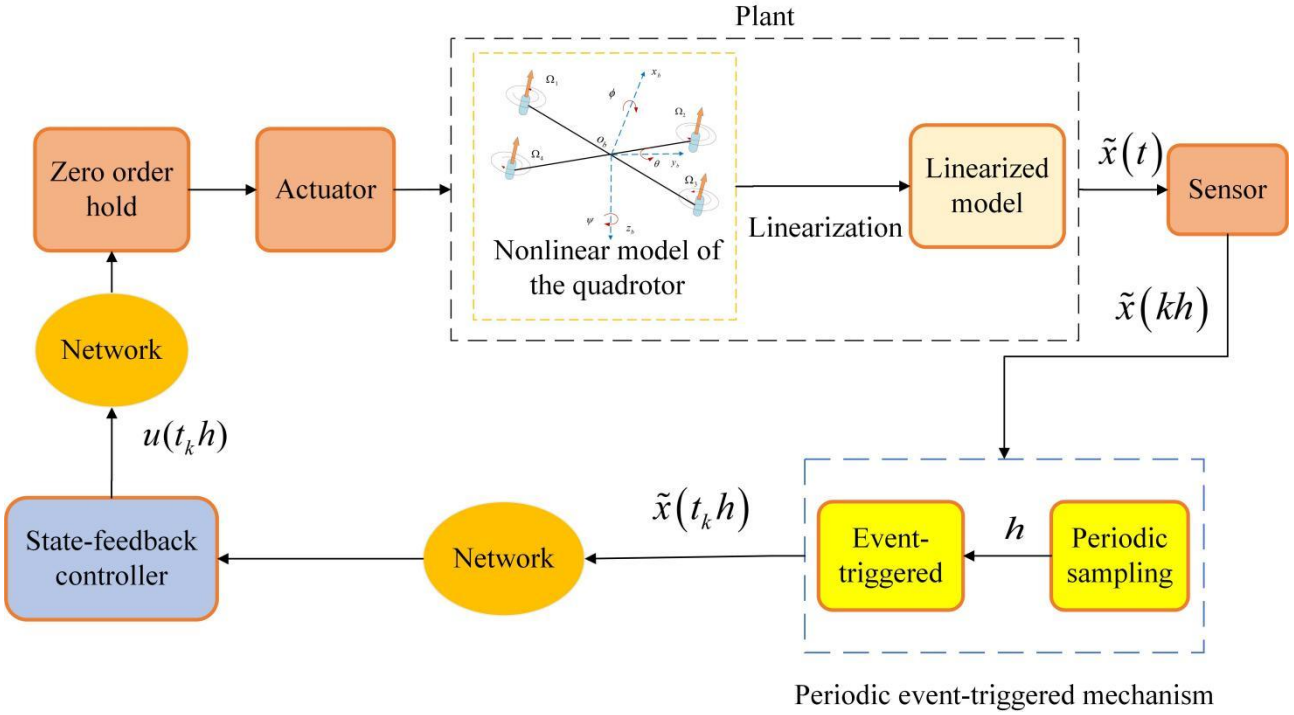

Figure 2: The quadrotor periodic event-triggered control schematic diagram.

The quadrotor periodic event-triggered control scheme is shown in Figure 2, and the specific design are as follows.

According to the quadrotor linear model (9), it can be rewritten as

$$\dot{\hat{x}}(t) = A\hat{x}(t) + Bu(t) \tag{14}$$

where $\hat{x}(t) \in \hat{R}^{12}$ and $u(t) \in \hat{R}^{4}$ represent the quadrotor system state vector and the control in put vector, respectively. $A \in \hat{R}^{12\times12}$ and $B \in \hat{R}^{12\times4}$ are constant matrices.

Design state feedback control law

$$u(t) = K\hat{x}(t_k h), t \in [t_k h, t_{k+1} h), k = 0,1,2\ldots, \tag{15}$$

$K \in \hat{R}^{4\times12}$ is the feedback gain matrix to be designed.

The state error is shown as

$$e_k(t) = \hat{x}(t_k h) - \hat{x}(t_k h + ih), t \in I_i, i = 0,1,\ldots,\hat{m}-1 \tag{16}$$

The event condition is constructed as

$$\left[\hat{x}(t_k h) - \hat{x}(t_k h + jh)\right]^T S_1 \left[\hat{x}(t_k h) - \hat{x}(t_k h + jh)\right] > \hat{x}^T(t_k h + jh) S_2 \hat{x}(t_k h + jh), \quad j = 0,1,\ldots, \tag{17}$$

where parameters S_1 and S_2 are positive definite matrices to be found.

ISSN: 2664-9640

In addition, the periodic event-triggered strategy determines whether an event is triggered at the moment of a fixed period, so there must be a minimum time interval (that is, the sampling time h) to avoid the occurrence of Zeno phenomenon.

In the existing literature, the common event conditions are as follows

$$\left[\hat{x}(t_k h)-\hat{x}(t_k h+jh)\right]^T \hat{\Omega}\left[\hat{x}(t_k h)-\hat{x}(t_k h+jh)\right] > \sigma \hat{x}^T(t_k h+ih)\hat{\Omega}\hat{x}(t_k h+ih), \quad j=0,1,\ldots, \tag{18}$$

where $\hat{\Omega}$ is a symmetric positive definite matrix and $\sigma \in [0,1)$ is the given trigger parameter, which is used to adjust the difficulty degree of event-triggered. When $\sigma = 0$ is periodic sampling control. Comparing the event condition (17) with the event condition (18) shows that the parameter matrices S_1 and S_2 are more general forms of the parameter matrices $\hat{\Omega}$ and $\sigma\hat{\Omega}$. Therefore, event condition (18) is a special form of event condition (17).

3.3. Jointing co-design criteria for the quadrotor system

[11] provided a design method for periodic event-triggered and state-feedback control of general linear systems. For this approach, we design a joint co-design criterion for the periodic event-triggered and state-feedback control of the quadrotor.

Algorithm 1 Jointing co-design criteria for quadrotor

1: The quadrotor system (14) is modeled and its controllability is judged.

2: The state-feedback control law (15), the state error (16), the event condition (17) and the sampling period h are defined.

3: On the basis of the step 2, the parameters $\alpha > 0, \beta > 0$ and matrix $\overline{E} > 0, \overline{F} > 0, \overline{R} > 0$, $\overline{S_1} > 0$, $\overline{S_2} > 0$, $Y = \begin{bmatrix} Y_{11} & Y_{12} \\ * & Y_{22} \end{bmatrix} \geq 0$, $\overline{N} = \left[\overline{N}_1^T, \overline{N}_2^T\right]^T$, $\overline{J} = \left[\overline{J}_1^T, \overline{J}_2^T\right]^T$, G, U with appropriate dimensions satisfying LMIs (19) and (20), where $S_1 = G^{-1}\overline{S}_1\left(G^T\right)^{-1}, S_2 = G^{-1}\overline{S}_2\left(G^T\right)^{-1}$ and $K = V\left(G^T\right)^{-1}$.

4: The parameters and matrix given in the step 3 satisfies LMIs, then the stability of the quadrotor system can be guaranteed and the state-feedback gain matrix K and the event condition parameters S_1 and S_2 can be obtained.

5: In the sampling period h, the system state is sampled and whether it meets the event condition (17) is judged.

6: If the event condition is met, the event triggers and updates the control law (15), then go to the next sampling period. If the event condition (17) is not met, going straight to the next sampling period.

$$\overline{\Gamma}_1 = \begin{bmatrix} \overline{\gamma}_{11} & \overline{\gamma}_{12} & -\overline{N}_1 & \overline{\gamma}_{14} & \eta BU \\ * & \overline{\gamma}_{22} & -\overline{N}_2 & \overline{\gamma}_{24} & \delta BU \\ * & * & -\overline{F}^* & 0 & 0 \\ * & * & * & \overline{\gamma}_{44} & BU \\ * & * & * & * & -\overline{S}_1 \end{bmatrix} < 0, \tag{19}$$

ISSN: 2664-9640

$$\bar{\Gamma}_2 = \begin{bmatrix} Y & \bar{I} \\ * & \bar{R} \end{bmatrix} \geq 0, \bar{\Gamma}_3 = \begin{bmatrix} Y & \bar{J} \\ * & \bar{R} \end{bmatrix} \geq 0, \tag{20}$$

where

$$\begin{aligned} \bar{\gamma}_{11} &= \bar{F} + \bar{J}_1 + \bar{J}_1^T + \alpha AG^T + \alpha GA^T + hY_{11}, \\ \bar{\gamma}_{12} &= \bar{N}_1 - \bar{J}_1 + \bar{J}_2^T + \alpha BU + \beta GA^T + hY_{12}, \\ \bar{\gamma}_{14} &= \bar{E} - \alpha G^T + GA^T, \\ \bar{\gamma}_{22} &= \bar{N}_2 + \bar{N}_2^T - \bar{J}_2 - \bar{J}_2^T + \beta BU + \beta U^T B^T + hY_{22} + \bar{S}_2, \\ \bar{\gamma}_{24} &= -\beta G^T + U^T B^T, \\ \bar{\gamma}_{44} &= h\bar{R} - G^T - G. \end{aligned} \tag{21}$$

then system (14) with control law (16) and event condition (17) is asymptotically stable.

4. Simulation

In this section, the feasibility and effectiveness of the proposed quadrotor control scheme is verified by simulation in MATLAB. The linear model of the system (9) has been given and the specific physical parameters of the quadrotor are given in Table 1. According to equation (14) and Table 1 , the A and B matrices of the quadrotor system model (9) are as follows.

Table 1: Specific physical parameters of the quadrotor system.

parameter	value	unit head
m	1.25	kg
g	9.8	m/s^2
J_x	0.0087	$kg \cdot m^2$
J_y	0.0087	$kg \cdot m^2$
J_z	0.0163	$kg \cdot m^2$

Source: The physical parameters of the quadrotor system are derived from [16].

$$A = \begin{bmatrix} 0 & 0 & 0 & 1 & 0 & 0 & 0 & 0 & 0 & 0 & 0 & 0 \\ 0 & 0 & 0 & 0 & 1 & 0 & 0 & 0 & 0 & 0 & 0 & 0 \\ 0 & 0 & 0 & 0 & 0 & 1 & 0 & 0 & 0 & 0 & 0 & 0 \\ 0 & 0 & 0 & 0 & 0 & 0 & 0 & -9.8 & 0 & 0 & 0 & 0 \\ 0 & 0 & 0 & 0 & 0 & 0 & 9.8 & 0 & 0 & 0 & 0 & 0 \\ 0 & 0 & 0 & 0 & 0 & 0 & 0 & 0 & 0 & 0 & 0 & 0 \\ 0 & 0 & 0 & 0 & 0 & 0 & 0 & 0 & 0 & 1 & 0 & 0 \\ 0 & 0 & 0 & 0 & 0 & 0 & 0 & 0 & 0 & 0 & 1 & 0 \\ 0 & 0 & 0 & 0 & 0 & 0 & 0 & 0 & 0 & 0 & 0 & 1 \\ 0 & 0 & 0 & 0 & 0 & 0 & 0 & 0 & 0 & 0 & 0 & 0 \\ 0 & 0 & 0 & 0 & 0 & 0 & 0 & 0 & 0 & 0 & 0 & 0 \\ 0 & 0 & 0 & 0 & 0 & 0 & 0 & 0 & 0 & 0 & 0 & 0 \end{bmatrix} \quad B = \begin{bmatrix} 0 & 0 & 0 & 0 \\ 0 & 0 & 0 & 0 \\ 0 & 0 & 0 & 0 \\ 0 & 0 & 0 & 0 \\ 0 & 0 & 0 & 0 \\ -0.8 & 0 & 0 & 0 \\ 0 & 0 & 0 & 0 \\ 0 & 0 & 0 & 0 \\ 0 & 0 & 0 & 0 \\ 0 & 114.94 & 0 & 0 \\ 0 & 0 & 114.94 & 0 \\ 0 & 0 & 0 & 61.35 \end{bmatrix}$$

ISSN: 2664-9640

Set $\alpha = 0.5, \beta = 0.2$ and $\sigma = 0.01$. When $h = 0.005s$ [17], the feedback gain matrix and event condition parameters are obtained by solving LMIs (19) and (20). Then, the obtained feedback gain matrix is taken as a common feedback gain matrix and the same verification period $\boldsymbol{h}$ is selected and brought into the event condition (18), and the corresponding event condition parameter $\hat{\Omega}$ can be obtained. Finally, the results in this paper are compared with those in the form of event condition (18).

$$K = \begin{bmatrix} 0 & 0 & 0.5949 & 0 & 0 & 1.6855 & 0 & 0 & 0 & 0 & 0 & 0 \\ 0 & -0.0018 & 0 & 0 & -0.0072 & 0 & -0.0964 & 0 & 0 & -0.0538 & 0 & 0 \\ 0.0018 & 0 & 0 & 0.0072 & 0 & 0 & 0 & -0.0964 & 0 & 0 & -0.0538 & 0 \\ 0 & 0 & 0 & 0 & 0 & 0 & 0 & 0 & -0.0078 & 0 & 0 & -0.0220 \end{bmatrix}$$

$$S1 = \begin{bmatrix} 0.5374 & 0 & 0 & 1.7521 & 0 & 0 & 0 & -20.6110 & 0 & 0 & -8.3474 & 0 \\ 0 & 0.5374 & 0 & 0 & 1.7521 & 0 & 20.6110 & 0 & 0 & 8.3474 & 0 & 0 \\ 0 & 0 & 0.0353 & 0 & 0 & 0.0773 & 0 & 0 & 0 & 0 & 0 & 0 \\ 1.7521 & 0 & 0 & 5.7575 & 0 & 0 & 0 & -67.9824 & 0 & 0 & -27.8695 & 0 \\ 0 & 1.7521 & 0 & 0 & 5.7575 & 0 & 67.9824 & 0 & 0 & 27.8695 & 0 & 0 \\ 0 & 0 & 0.0773 & 0 & 0 & 0.2107 & 0 & 0 & 0 & 0 & 0 & 0 \\ 0 & 20.6110 & 0 & 0 & 67.9824 & 0 & 806.0042 & 0 & 0 & 333.4228 & 0 & 0 \\ -20.6110 & 0 & 0 & -67.9824 & 0 & 0 & 0 & 806.0042 & 0 & 0 & 333.4228 & 0 \\ 0 & 0 & 0 & 0 & 0 & 0 & 0 & 0 & 0.0353 & 0 & 0 & 0.0773 \\ 0 & 8.3474 & 0 & 0 & 27.8695 & 0 & 333.4228 & 0 & 0 & 142.0622 & 0 & 0 \\ -8.3474 & 0 & 0 & -27.8695 & 0 & 0 & 0 & 333.4228 & 0 & 0 & 142.0622 & 0 \\ 0 & 0 & 0 & 0 & 0 & 0 & 0 & 0 & 0.0773 & 0 & 0 & 0.2107 \end{bmatrix}$$

$$S2 = \begin{bmatrix} 0.0012 & 0 & 0 & 0.0032 & 0 & 0 & 0 & -0.0387 & 0 & 0 & -0.0197 & 0 \\ 0 & 0.0012 & 0 & 0 & 0.0032 & 0 & 0.0387 & 0 & 0 & 0.0197 & 0 & 0 \\ 0 & 0 & 0.0033 & 0 & 0 & 0.0055 & 0 & 0 & 0 & 0 & 0 & 0 \\ 0.0032 & 0 & 0 & 0.0145 & 0 & 0 & 0 & -0.1518 & 0 & 0 & -0.0870 & 0 \\ 0 & 0.0032 & 0 & 0 & 0.0145 & 0 & 0.1518 & 0 & 0 & 0.0870 & 0 & 0 \\ 0 & 0 & 0.0055 & 0 & 0 & 0.0195 & 0 & 0 & 0 & 0 & 0 & 0 \\ 0 & 0.0387 & 0 & 0 & 0.1518 & 0 & 1.8078 & 0 & 0 & 0.9872 & 0 & 0 \\ -0.0389 & 0 & 0 & -0.1518 & 0 & 0 & 0 & 1.8078 & 0 & 0 & 0.9872 & 0 \\ 0 & 0 & 0 & 0 & 0 & 0 & 0 & 0 & 0.0033 & 0 & 0 & 0.0055 \\ 0 & 0.0197 & 0 & 0 & 0.0870 & 0 & 0.9872 & 0 & 0 & 0.5955 & 0 & 0 \\ -0.0197 & 0 & 0 & -0.0870 & 0 & 0 & 0 & 0.9872 & 0 & 0 & 0.5955 & 0 \\ 0 & 0 & 0 & 0 & 0 & 0 & 0 & 0 & 0.0055 & 0 & 0 & 0.0195 \end{bmatrix}$$

$$\hat{\Omega} = \begin{bmatrix} 1.3466 & 0 & 0 & 0.1919 & 0 & 0 & 0 & -3.3129 & 0 & 0 & -1.4768 & 0 \\ 0 & 1.3466 & 0 & 0 & 0.1919 & 0 & 3.3129 & 0 & 0 & 1.4768 & 0 & 0 \\ 0 & 0 & 37.5537 & 0 & 0 & 7.8398 & 0 & 0 & 0 & 0 & 0 & 0 \\ 0.1919 & 0 & 0 & 6.7933 & 0 & 0 & 0 & -10.6925 & 0 & 0 & -8.2381 & 0 \\ 0 & 0.1919 & 0 & 0 & 6.7933 & 0 & 10.6925 & 0 & 0 & 8.2381 & 0 & 0 \\ 0 & 0 & 7.8398 & 0 & 0 & 58.4803 & 0 & 0 & 0 & 0 & 0 & 0 \\ 0 & 3.3129 & 0 & 0 & 10.6925 & 0 & 178.5319 & 0 & 0 & 79.8196 & 0 & 0 \\ -3.3129 & 0 & 0 & 10.6925 & 0 & 0 & 0 & 178.5319 & 0 & 0 & 79.8196 & 0 \\ 0 & 0 & 0 & 0 & 0 & 0 & 0 & 0 & 37.5874 & 0 & 0 & 7.8642 \\ 0 & 1.4768 & 0 & 0 & 8.2381 & 0 & 79.8196 & 0 & 0 & 80.5087 & 0 & 0 \\ -1.4768 & 0 & 0 & 8.2381 & 0 & 0 & 0 & 79.8196 & 0 & 0 & 80.5087 & 0 \\ 0 & 0 & 0 & 0 & 0 & 0 & 0 & 0 & 7.8642 & 0 & 0 & 58.4494 \end{bmatrix}$$

The state trajectory with event condition (17) and (18) is shown in Figures 3 and 4.

ISSN: 2664-9640

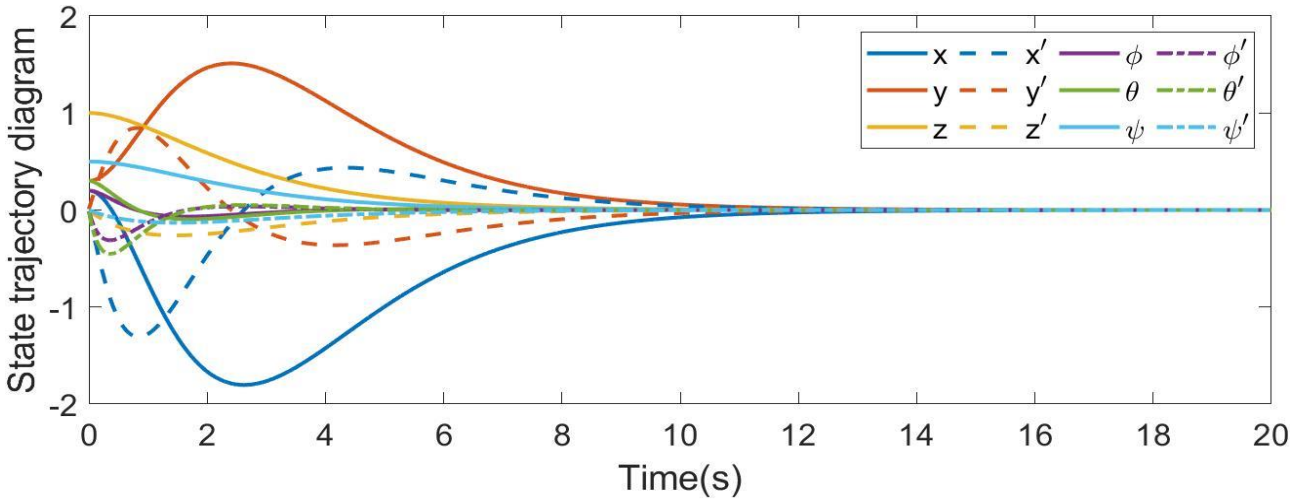

Figure 3: The state trajectories using event conditions (17).

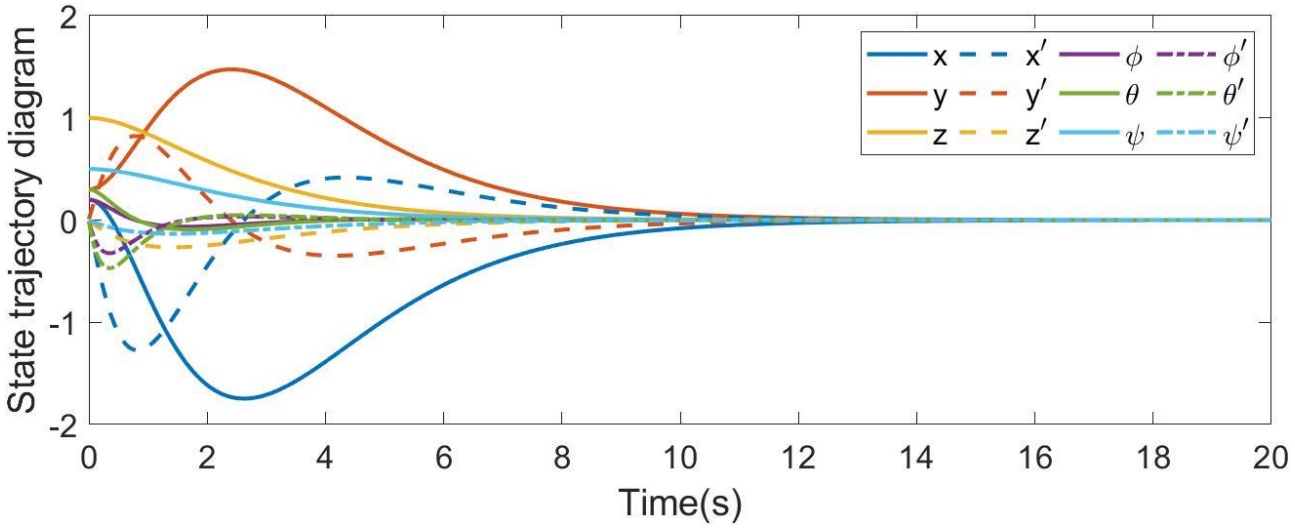

Figure 4: The state trajectories using event conditions (18).

By comparison, the stability time of the state trajectory in event condition (17) is essentially the same as in event condition (18) .

The event-triggered interval with event conditions (17) and (18) is shown in Figures 5 and 6.

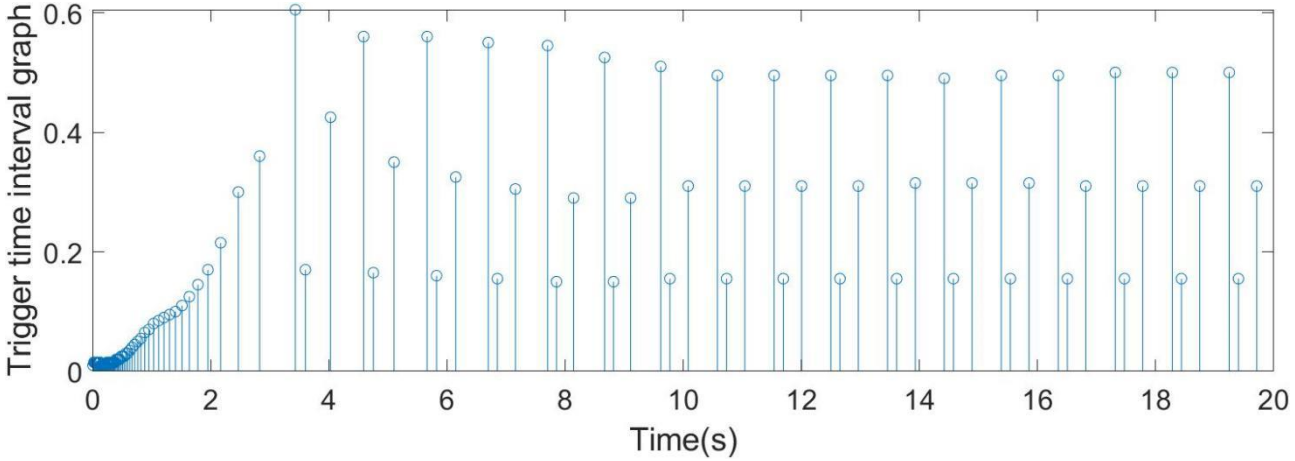

Figure 5: The inter-event times under event condition (17).

ISSN: 2664-9640

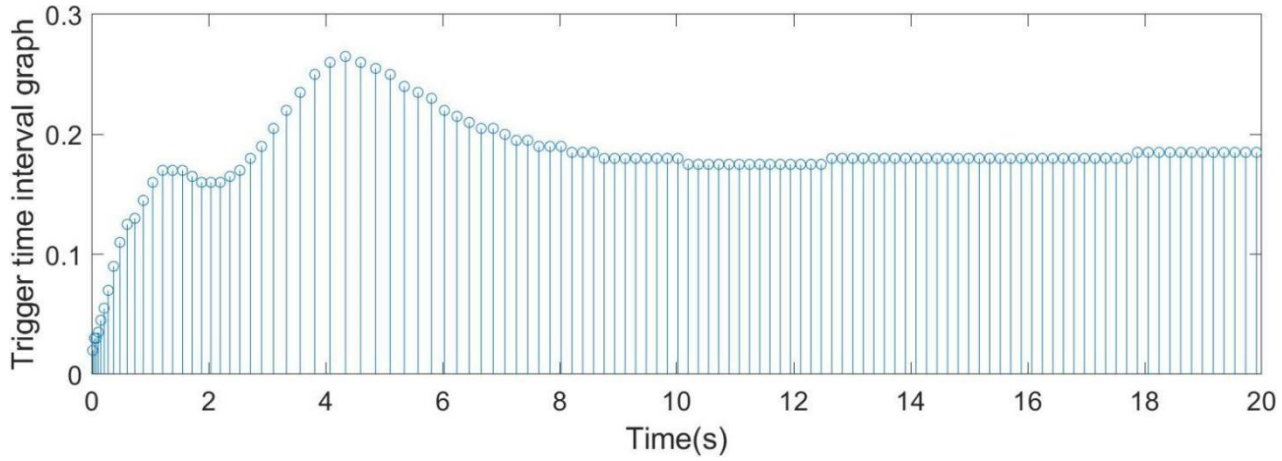

Figure 6: The inter-event times under event condition (18).

The average interval between events under event condition (17) is 0.1825s and the number of events triggered is 108. The average interval between events under event condition (18) is 0.1762s and the number of events triggered is 113. Therefore, it can be obtained that under the same verification cycle and communication time, the event condition (17) saves 5 times of communication calculation for control law updating compared to the event condition (18). The simulation time is 20s and the verification period is 0.005s, so there are 4001 sampling points in total. In the control scheme designed in this paper, the number of triggered events is 108 and the controller update rate is 3%, which significantly reduces the number of controller updates compared with the traditional state feedback controller.

Through the above simulation analysis, it can be seen that the control scheme designed in this paper has better ability to save communication resources than the control scheme under event condition (18) without affecting the performance of the controller.

According to the simulation data, we conducted a three-dimensional simulation of the flight trajectory of the quadrotor aircraft, as shown in Figure 7.

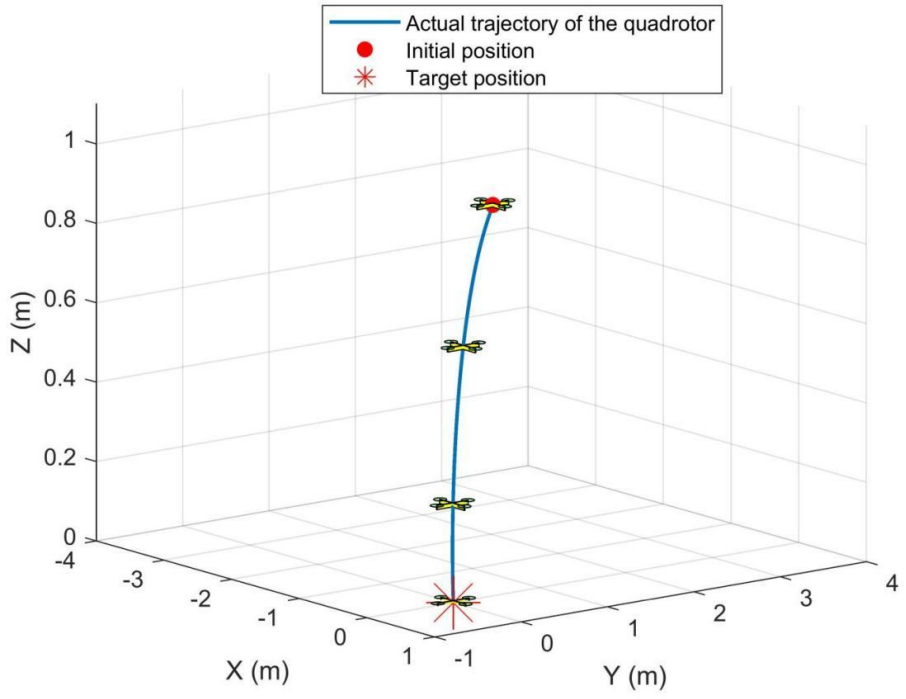

Figure 7: The trajectory of the quadrotor is simulated in 3D.

ISSN: 2664-9640

5. Conclusion

In this paper, a control scheme combining periodic event-triggered mechanism and the quadrotor state-feedback controller is designed. To save communication resources and avoid Zeno phenomena, periodic event-triggered control is employed. The designed event condition (17) has a more general form than (18). Simulation results show that the periodic event-triggered control strategy proposed in this paper saves more resources than the event condition (18).

In the future, we will study the periodic event-triggered control strategy based on output-feedback. In addition, when this control scheme is applied to drone swarm, the communication environment becomes more complex, a topic we will address in our next work.

Acknowledgements

The authors thank the anonymous reviewers for their valuable suggestions. The authors have declared that no conflict of interest exists.

References

[1] Moad Idrissi, Mohammad Salami and Fawaz Annaz. A Review of Quadrotor Unmanned Aerial Vehicles: Applications, Architectural Design and Control Algorithms [J]. Journal of Intelligent & Robotic Systems, 2022, 104(2):1-33.

[2] Wu Di, Zhang Weijian, Du Haibo, Wang Xiangyu. Robust adaptive finite-time trajectory tracking control of a quadrotor aircraft. International Journal of Robust and Nonlinear Control, 2021.

[3] Lin Xiaobo, Liu Jian, Yu Yao, Sun Changyin. Event-triggered reinforcement learning control for the quadrotor UAV with actuator saturation[J]. Neurocomputing, 2020,415:135-145.

[4] Yue Jiangfeng, Qin Kaiyu, Shi Mengji, Jiang Bing, Li Weihao, Shi Lei. Event-Trigger-Based Finite-Time Privacy-Preserving Formation Control for Multi-UAV System[J]. Drones, 2023,7(4):235,.

[5] Wang Wu, Guo Junyou, Tian Guoqing, Chen Yutao, Huang Jie. Event-Triggered Intervention Framework for UAV-UGV Coordination Systems[J]. Machines, 2021, 9(12):371 .

[6] Ni Wei, Zhao Ping, Wang Xiaoli, Wang Jinhuan. Event-triggered control of linear systems with saturated inputs. Asian Journal of Control, 2015.

[7] Yazdan Batmani. A Decentralized Event-Triggered State-Feedback Control Technique for Continuous-Time Linear Systems. IEEE Transactions on Systems, Man, and Cybernetics: Systems, 53, 2023.

[8] Shao Shuyi, Chen Mou, Hou Jie, Zhao Qijun. Event-triggered-based discrete-time neural control for a quadrotor UAV using disturbance observer[J]. IEEE/ASME Transactions on Mechatronics, 2021,PP(99):1-1 .

[9] Zhang Min, Ding Zhengtao, Huang Jing, Huang Tingxuan. Tracking control for unmanned aerial vehicles with time-delays based on event-triggered mechanism[J]. Journal of Control Engineering and Applied Informatics, 2019, 21(3):12–19.

[10] Wu Zhiying, Xiong Junlin, Xie Min. A Switching Method to Event-Triggered Output Feedback Control for Unmanned Aerial Vehicles Over Cognitive Radio Networks[J]. IEEE Transactions on Systems, Man, and Cybernetics: Systems, 2021, 51(12):7530–7541 .

[11] Chen Xia, Hao Fei. Periodic event-triggered state-feedback and output-feedback control for linear systems[J]. International Journal of Control, Automation and Systems, 2015, 13(4):779–787 .

[12] Quan Quan. Introduction to multicopter design and control. Springer, 2017.

[13] W.P.M.H. Heemels, M.C.F. Donkers and A.R. Teel. Periodic event-triggered control based on state-feedback. Proc of the 50th IEEE CDC/ECC. Orlando: IEEE, 2571-2576, 2011.

[14] J.L.C. Verhaegh, T.M.P. Gommans and W.P.M.H. Heemels. Extension and evaluation of model-based periodic event-triggered control. Control Conference, 2012.

ISSN: 2664-9640

[15] W.P.M.H. Heemels, M.C.F.Donkers and A.R. Teel. Periodic event-triggered control for linear systems. IEEE 52nd Annual Conference on Decision and Control (CDC) (Vol.58), IEEE, 2013.

[16] Zhang Dong, Yang Yunxiao, Han Hengzhi, Hu Yubin. Binocular visual pendulum angle detection and anti-swing control of quadrotor suspension system[J]. Transactions of the Institute of Measurement and Control, 2023, 45(4):723–735.

[17] Wu Tong, Wang Jie, Tian Bailing. Periodic event-triggered formation control for multi-UAV systems with collision avoidance[J]. Chinese Journal of Aeronautics, 2022, 35(8):11 .

[18] Xi Houyin, Zhang Dong, Zhou Tao, Yang Yunxiao, Wei Qiang. An anti-wind modeling method of quadrotor aircraft and cascade controller design based on improved extended state observer[J]. International Journal of Control, Automation and Systems, 2021, 19:1363–1374.